Dual-Targeting of β -Tubulin and Carbonic Anhydrase IX by Albendazole-Etoricoxib Combination Induces Synergistic Cytotoxicity and Energetic Strangulation in Cervical Cancer Cells

Sura Findakly[1], Aiad Gaber Arean[2,*], Saba Jesem Alheshemi[3] and Henan Dh. Skheel Aljebori[1]

[1]*College of Medicine, Al-Mustansiriyah University, Iraq*

[2]*Department of Medical Chemistry, College of Medicine, Al-Muthanna University, Iraq*

[3]*Department of Gynecology and Obstetrics, Medical College Misan University, Iraq*

Abstract: *Objective:* This study was performed to evaluate the cytotoxic effects and synergistic interactions of Albendazole combined with Etoricoxib on HeLa cervical carcinoma cells, emphasizing mechanisms involving disruption of glycolytic metabolism and cellular pH regulation.

Materials and Methods: The study investigated the cytotoxic effects of Albendazole, Etoricoxib, their combination, and 5-Fluorouracil (5-FU) on HeLa cells and normal human foreskin fibroblasts (HFF) via MTT assays. It also calculated the Combination Index (CI) and Dose Reduction Index (DRI) using CompuSyn software to evaluate drug synergy. Furthermore, lactate production and carbonic anhydrase activity were measured to analyze glycolytic flux and pH regulation, and were complemented by molecular docking of the drugs with β-tubulin and carbonic anhydrase IX.

Results: The combination of Albendazole and Etoricoxib exhibited significant synergistic cytotoxic effects against HeLa cells, compared to either agent alone or 5-Fluorouracil (5-FU). The combination also showed high selectivity, indicating a sparing impact on HFF cells, unlike 5-FU. Furthermore, the combined treatment markedly inhibited lactate production by 85.1% and carbonic anhydrase activity by 86.3%. Molecular docking studies corroborated these findings by revealing stable binding interactions of Albendazole with β-tubulin and Etoricoxib with CA-IX, with docking scores of -6.7 and -7.1 kcal/mol, respectively, supporting a dual-targeting mechanism.

Conclusion: The combined use of Albendazole and Etoricoxib produces a synergistic effect on cervical cancer cells by disrupting glycolytic metabolism and cellular pH regulation. This targeted approach offers a promising way to overcome chemoresistance and lessen toxicity, thereby improving therapeutic effectiveness in cervical cancer treatment.

Keywords: Albendazole, Etoricoxib, Cervical Cancer, Drug Synergy, Energetic Strangulation, Glycolysis, Carbonic Anhydrase IX, β-tubulin, Drug Repurposing.

1. INTRODUCTION

Cervical carcinoma continues to represent a significant public health concern globally, ranking as the fourth most prevalent cancer and the leading cause of oncologic mortality among women [1]. High-income nations have experienced a reduction in the prevalence of HPV-related diseases, attributable to comprehensive vaccination and screening initiatives. Conversely, women in low- and middle-income countries remain disproportionately affected, owing to the restricted availability of preventive healthcare services [2, 3]. For patients presenting with advanced, recurrent, or metastatic disease, the primary therapeutic approach generally involves administering platinum-based chemotherapeutic agents, such as 5-fluorouracil (5-FU), often in combination with other agents [4, 5]. However, the clinical efficacy of these regimens is frequently hindered by the development of acquired chemoresistance and notable systemic toxicities, both of which limit dosage and significantly impair patients' quality of life [6].

Chemotherapy resistance constitutes a significant obstacle in the management of cervical cancer, frequently resulting in disease recurrence and suboptimal prognoses. To mitigate this issue, drug repurposing—defined as the application of existing pharmacological agents with well-established safety profiles, initially developed for non-oncological indications—has gained prominence as a viable strategy to enhance therapeutic efficacy. This approach accelerates the drug development process and reduces associated costs. Currently, antidiabetic and antiparasitic agents represent the most extensively studied candidates for repurposing in this context [7-16].

Albendazole, a drug traditionally employed as an anthelmintic agent, has garnered increasing interest for its potential application as an anticancer therapeutic. As a broad-spectrum benzimidazole derivative, it was initially synthesized to disrupt parasite microtubules by

*Address correspondence to these authors at the Department of Medical Chemistry, College of Medicine, Al-Muthanna University, Iraq;
E-mail: aiadgaber@mu.edu.iq

ISSN: 1929-2260 / E-ISSN: 1929-2279/26

inhibiting β-tubulin polymerization. This mechanism appears to exert significant anti-proliferative effects on mammalian cancer cells. Preclinical investigations have demonstrated that albendazole can mitigate tumor progression across various models, including hepatocellular carcinoma, ovarian carcinoma, prostate cancer, and colorectal carcinoma, predominantly through the induction of mitotic arrest and apoptosis [17, 18]. Its functions include inhibiting angiogenesis and enhancing radiosensitivity, underscoring its multifaceted antineoplastic properties [19, 20].

Furthermore, Etoricoxib, a selective inhibitor of cyclooxygenase-2 (COX-2], has attracted scholarly interest for its potential antineoplastic properties beyond its conventional anti-inflammatory function. COX-2 is commonly overexpressed in numerous malignancies, and its inhibition has been associated with the suppression of tumor proliferation and angiogenesis [21-23]. Furthermore, emerging evidence suggests that the anticancer mechanisms of etoricoxib may extend beyond prostaglandin suppression. Notably, it has demonstrated the ability to disrupt critical metabolic pathways in cancer cells, including inhibition of glycolytic flux and modulation of pH-regulatory enzymes, such as carbonic anhydrase IX (CA-IX) [22, 24]. This multifaceted approach designates etoricoxib as a promising candidate for drug repurposing in oncology.

Although promising, the individual limitations of these agents underscore the need for a combination strategy. When used as monotherapies, Albendazole often demonstrates a high IC_{50}, which may restrict its clinical effectiveness against solid tumors. Similarly, Etoricoxib's primary anti-inflammatory function may not provide sufficient anticancer activity on its own. These limitations underscore that their isolated use could be suboptimal, providing a compelling rationale for exploring their potential synergistic effects to enhance cytotoxicity and address individual shortcomings.

The development of effective cancer therapies is increasingly focused on targeting essential biological processes that drive tumor progression. Among these, the β-tubulin subunit of microtubules and carbonic anhydrase IX (CA-IX) are particularly significant, as they regulate the "Growth Hub" and "Power Hub" mechanisms within cancer cells, respectively. Microtubules, predominantly composed of β -tubulin, fulfill roles that transcend mere structural support. They are essential for critical cellular processes, including mitosis and intracellular trafficking, and are instrumental in the spatial organization of glycolytic enzymes. This organizational capacity is directly linked to the metabolic reprogramming commonly observed in neoplastic cells [25, 26]. The tumor microenvironment is frequently characterized by acidity and hypoxia, conditions that strongly induce carbonic anhydrase IX (CA-IX) upregulation. This enzyme functions as a crucial regulator of pH homeostasis; it catalyzes the hydration of carbon dioxide, thereby maintaining an optimal intracellular pH. Concurrently, it contributes to acidification of the extracellular milieu, thereby facilitating tumor invasion, metastasis, and resistance to chemotherapy [22, 24, 27].

We propose that a strategy combining β-tubulin inhibition, which disrupts cellular division and metabolic coordination, with targeting carbonic anhydrase IX (CA-IX), which impairs the cell's capacity to regulate metabolic acidosis, may constitute a practical therapeutic approach. This dual modality compromises both structural integrity and pH homeostasis, thereby offering a promising avenue for selectively inducing synthetic lethality in malignant cells.

While the individual anticancer properties of Albendazole and Etoricoxib have been examined to some extent, the potential synergistic cytotoxic effects of their combination remain underexplored, particularly in cervical carcinoma. Existing research has established the roles of Albendazole in microtubule disruption and of Etoricoxib as a COX-2 inhibitor with emerging metabolic effects. However, a significant gap remains in understanding the mechanistic basis and therapeutic potential of their combined application. In particular, it is unclear whether concurrent targeting of the β -tubulin "Growth Hub" with Albendazole and the Carbonic Anhydrase IX (CA-IX) "Power Hub" with Etoricoxib can induce synergistic "energetic strangulation" in cancer cells, thereby simultaneously impairing cellular structural integrity, glycolytic activity, and pH regulation. Additionally, the cytotoxic selectivity of this combination against cervical cancer cells, compared with normal cells and relative to standard chemotherapeutics such as 5-Fluorouracil (5-FU), has not been systematically investigated. This study aims to address this gap by systematically evaluating the synergistic cytotoxic effects, metabolic disruptions, and molecular binding interactions associated with the Albendazole-Etoricoxib combination.

2. MATERIALS AND METHODS

2.1. Cytotoxic Assay

2.1.1 Medications and Tissue Culture

Medications, including Albendazole, etoricoxib, and 5-FU, were obtained as raw materials from the

Samarra Pharmaceutical Factory in Iraq. These substances, along with a mixture of (Albendazole – etoricoxib), were diluted in Minimum Essential Medium (MEM) to achieve concentrations ranging from 0.1 to 1000 µg/mL. Specifically, within the mixture, the concentrations of Albendazole and etoricoxib ranged from 0.05 to 50 µg/mL, resulting in a final concentration range of 0.1 to 1000 µg/mL.

The cytotoxicity of the tested compounds was evaluated on the human cervical carcinoma cell line HeLa to assess their anticancer efficacy. The compounds investigated included Albendazole, etoricoxib, 5-Fluorouracil (5-FU), and the mixture. Furthermore, the study examined the effects of the mixture on normal human foreskin fibroblasts (HFFs), which serve as a model for non-malignant tissue, to determine its safety profile and potential impact on cell viability.

Furthermore, the cytotoxicity and safety profiles of these agents were evaluated by assessing cell viability across a concentration range of 0.1-1000 µg/mL in both malignant and normal cell lines. The cell lines used in this study were obtained from the Tissue Culture Unit at the Iraqi Center for Cancer and Medical Genetics Research at Al-Mustansiriyah University.

2.1.2. Study Cell Lines and Culture Conditions

The study employed two cell lines, one of which was HeLa, derived from human cervical carcinoma tissue [28, 29]. The healthy, normal cell line (HFF) is derived from human foreskin fibroblasts [30]. MEM medium from US Biological (USA) was used for cell culture, supplemented with 10% (v/v) fetal bovine serum (FBS) from Capricorn Scientific (Germany), and 100 IU/mL of penicillin and 100 µg/mL of streptomycin to prevent bacterial contamination. The cells were cultured in a humidified incubator maintained at 37°C throughout the exponential growth phase [31].

2.1.3. Assessment of Cytotoxic Activity and IC_{50} Estimation

The MTT assay represents a widely utilized colorimetric method for assessing cellular metabolic viability. It is based on the reduction of the tetrazolium salt MTT by living cells to insoluble purple formazan crystals, a reaction primarily mediated by mitochondrial dehydrogenases. Typically, cells are cultured in 96-well plates and exposed to various concentrations of test compounds. After incubation for 24 or 72 hours, MTT reagent is added, and subsequent incubation allows the reagent to be reduced by viable cells. The resulting formazan is solubilized, and its absorbance is measured spectrophotometrically at a specific wavelength, providing a quantitative measure of cell viability [32].

This assay shows a clear correlation between viable cell count and formazan production. Pharmacological agent administration results in decreased formazan levels, indicating cytotoxicity, as evidenced by lower absorbance readings. The dose-response curve is used to determine the IC50, the drug concentration that reduces cell viability by 50%. This parameter was calculated using GraphPad Prism software (version 9.5.0, build 750) [33, 34].

Cells were seeded into 96-well microplates at a density of 10,000 cells per well and incubated at 37°C for 24 hours until reaching confluence. The cytotoxic effects of Albendazole, Etoricoxib, 5-Fluorouracil (5-FU), and the mixture were evaluated using an MTT assay. Each concentration was tested in six replicate wells, with cells treated with various concentrations (0.1, 1, 10, 100, and 1000 µg/mL) alongside untreated controls in approximately 20 replicates. After 24 and 72 hours, 28 µL of 2 mg/mL MTT solution was added to each well, followed by a three-hour incubation. Subsequently, 100 µL of DMSO was added, and plates were incubated for an additional 15 minutes to dissolve formazan crystals. Absorbance was measured at 570 nm using a microplate reader, and cell viability was calculated using an appropriate formula [35].

$$Growth\ inhibition\ \% = \frac{optical\ density\ of\ control\ wells - optical\ density\ of\ treated\ wells}{optical\ density\ of\ control\ wells} * 100\%$$

2.2. Identification of Selective Cytotoxicity

The selective toxicity index was used to compare the cytotoxic selectivity of the Albendazole-Etoricoxib combination with that of 5-Fluorouracil (5-FU). This metric facilitated the assessment of cytotoxic effects in cancer cell lines after incubation for 24 and 72 hours. IC50 values for both the combination and 5-FU were calculated, and the selective cytotoxicity index was subsequently derived from growth curve analyses of HeLa cells and normal human foreskin fibroblasts (HFF). [36], as illustrated in the following mathematical equation

$$Selective\ toxicity\ Index\ (SI) = \frac{IC50\ of\ normal\ cell\ lines}{IC50\ of\ cancer\ cell\ lines}$$

An SI score greater than 1.0 signifies that a drug is more efficient at targeting tumor cells compared to normal cells.

2.3. Analysis of Drug Interaction: Combination Index and Dose Reduction Index

Compusyn, a computational simulation tool, was used to determine the combination index (CI) values and the dose reduction index (DRI). The primary objective of the CI was to determine whether the mixture components exhibited synergistic, additive, or antagonistic interactions. This involved analyzing concentration-effect curves, which illustrate the percentage inhibition of cell proliferation at different drug concentrations, measured at 24 and 72 hours post-treatment. Values of the combination index (CI) below 1 indicate synergism, a CI of exactly 1 signifies an additive effect, and a CI above 1 suggests antagonism. These calculations were carried out using Compusyn software (Biosoft, Ferguson, MO, USA) [37, 38].

Furthermore, an essential metric for evaluating drug combinations is the Dose Reduction Index (DRI), which quantifies the maximum achievable decrease in each drug's concentration in the mixture while maintaining cytotoxicity. A DRI score above 1 signifies a beneficial reduction in concentration, whereas a score below 1 indicates an undesirable decrease. The DRI analysis was performed using Compusyn software (Biosoft, Ferguson, MO, USA) [37, 38].

2.4. Morphological Assessment

Morphological alterations in HeLa and HFF cells were examined and documented after 72 hours of exposure to the test compounds using inverted light microscopy.

2.5. Evaluation of Glycolytic Rate and Carbonic Anhydrase Levels

To evaluate the effects of the study treatment on glycolytic rate and carbonic anhydrase levels, assays for lactate production and esterase activity were conducted.

2.5.1. Lactate Production Assessment

This assessment measured lactate levels in cell culture medium using a colorimetric Lactate Assay Kit (Abcam, ab65331) according to the manufacturer's protocol. It was used to determine the glycolytic rate. After the 24-hour treatment, 50 µL of cell culture supernatant from each well of treated and untreated HeLa and HFF cells was carefully collected without disrupting the cell monolayer. The collected samples were immediately stored at -80°C until further analysis.

The assay was conducted in a 96-well plate with clear wells. Briefly, 50 µL of each collected supernatant was combined with 50 µL of Lactate Assay Reaction Mix. The plate was incubated at room temperature for 30 minutes, protected from light. The absorbance of the resulting-colored product was measured at 570 nm using a BioTek Synergy H1 microplate reader. A standard curve with known lactate concentrations (0-10 nmol/well) was prepared in parallel to determine lactate concentrations in the samples. Results were normalized to total protein content, determined using a bicinchoninic acid (BCA) protein assay [39].

2.5.2. Esterase Activity Assay

The esterase activity of carbonic anhydrase (CA) in cell lysates was measured using 4-nitrophenyl acetate (4-NPA) as the substrate. Following a 24-hour treatment period, 50 µL of cell culture supernatant was carefully collected from each well of treated and untreated HeLa and HFF cells, ensuring the integrity of the cell monolayer was maintained. The samples were then immediately stored at -80°C pending further analysis.

After removing the culture medium designated for the lactate assay, the adherent cells cultured in 24-well plates were washed twice with ice-cold phosphate-buffered saline (PBS). Cells were subsequently lysed in situ with 100 µL of RIPA buffer supplemented with a protease inhibitor cocktail. The lysates were collected, incubated on ice for 15 minutes, and centrifuged at 12,000 × g for 15 minutes at 4°C to remove cellular debris. The resulting supernatants were used as a source of carbonic anhydrase (CA).

The enzymatic activity assay was performed in a 96-well plate. For each sample, 80 µL of cell lysate was mixed with 100 µL of assay buffer (20 mM Tris-HCl, pH 8.0). The reaction was initiated by adding 20 µL of the 4-nitrophenyl acetate (4-NPA) substrate (final concentration: 1 mM) prepared in acetonitrile. The increase in absorbance at 348 nm, indicative of 4-NPA hydrolysis to 4-nitrophenol, was monitored immediately at one-minute intervals over 10 minutes using a microplate reader. The reaction rate (Δ Absorbance/min) was determined from the linear segment of the kinetic curve. Protein concentration in the lysates was quantified via bicinchoninic acid (BCA) assay, and esterase activity was expressed as ΔA/min/mg of total protein [40].

2.6. Molecular Docking Assay

The structural models of Albendazole and Etoricoxib were built and optimized using ChemDraw (Cambridge

Soft, USA) and Chem3D software. To clarify the molecular basis of the proposed dual-mechanism action, computational docking studies were performed against two key targets. The first target was the human wild-type β-tubulin subunit, a core part of the "Growth Hub" that supports cell proliferation and intracellular transport. The second was Carbonic Anhydrase IX (CA-IX), a major regulator of the "Power Hub" that manages energy metabolism and microenvironmental pH to help tumor survival.

The selection of these two targets is based on their crucial roles in cancer. The human wild-type β-tubulin subunit plays a vital role in cancer biology beyond merely serving as a structural component of microtubules. While isotypes such as βIII-tubulin (TUBB3) are linked to chemoresistance, the overall pool of wild-type β-tubulin is significantly involved in tumor progression. Microtubules underpin essential cellular processes, including mitosis, intracellular trafficking, and motility—mechanisms exploited by cancer cells for growth and invasion. Notably, microtubules facilitate the transport of glucose transporters such as GLUT4 to the plasma membrane, linking β-tubulin integrity to cellular metabolism. Additionally, microtubules organize glycolytic enzymes into metabolons, enhancing glycolytic efficiency—a phenomenon characteristic of cancer's metabolic reprogramming known as the Warburg effect. Thus, wild-type β-tubulin is integral to both structural and metabolic functions in tumor cells, rendering it a validated target for anticancer therapies that disrupt microtubule dynamics [25, 26].

Moreover, Carbonic Anhydrase IX (CA-IX) is a tumor-specific enzyme that significantly modulates the tumor microenvironment. Its expression is primarily induced under hypoxic conditions via the HIF-1α pathway, leading to prominent plasma membrane localization in many solid tumors and minimal expression in normal tissues. CA-IX facilitates the reversible hydration of carbon dioxide to bicarbonate and protons, a process essential for cellular pH regulation. In malignant cells, this activity contributes to extracellular acidification, thereby promoting invasion, metastasis, and therapeutic resistance, whereas intracellular alkalization supports survival amid metabolic acidosis. Consequently, CA-IX plays a dual role: enhancing tumor progression by altering pH dynamics, making it a compelling target for anticancer therapeutics that disrupt tumor-specific pH homeostasis and limit tumor aggressiveness [22, 24].

This dual-targeting strategy enhances the disruption of malignant cells by simultaneously compromising structural integrity and pH regulation. Specifically, the approach involves inhibiting β-tubulin in the 'Growth Hub' with Albendazole to impair microtubule function and modulating the pH-regulatory enzyme CA-IX in the "Power Hub" with Etoricoxib to disrupt cellular pH homeostasis. This multifaceted intervention induces a synthetic energetic crisis in cancer cells by disrupting fuel transport, glycolytic activity, and mitochondrial membrane potential, exploiting the distinct metabolic dependencies and proliferative characteristics that differentiate transformed cells from normal tissue.

The three-dimensional structures of these critical cancer dependencies were obtained from the Protein Data Bank (PDB codes: 5C8Yfor human wild-type β-tubulin subunit and 5DVXfor Carbonic Anhydrase IX (CA-IX)). These structures were used in docking analyses because they represent constitutively active, disease-associated conformations, which are primary therapeutic targets in oncological contexts.

The selected PDB structures, 5C8Y for human wild-type β-tubulin and 5DVX for CA-IX, were selected for their high-resolution and disease-relevant conformations. Structure 5C8Y represents a native, polymerizable human β-tubulin isotype and serves as a validated model for studying antiproliferative drug binding. The 5DVX structure depicts CA-IX in its catalytically active form, which is essential for evaluating pH-regulatory inhibition. These particular entries offer optimal templates for assessing direct, therapeutically significant interactions within the context of the proposed dual-targeting strategy.

These critical dependencies in cancer pathogenesis were characterized using Auto Dock Tools. This process entailed identifying optimal ligand conformations and generating PDBQT files to facilitate subsequent analyses. Additionally, the molecular structures of Albendazole, Etoricoxib, the human wild-type β-tubulin subunit,and Carbonic Anhydrase were imported into Auto Dock Tools for docking. The resulting datasets, comprising binding energy scores and interaction profiles, were systematically analyzed using BIOVIA Discovery Studio, UCSF Chimera, and AutoDock software suites [41, 42].

2.7. Ethical Approval

Our investigation was confined to *in vitro* cell line models and did not incorporate human subjects or laboratory animals. Nevertheless, we maintained full

compliance with our institution's ethical standards governing laboratory research throughout the study.

2.8. Statistical Analysis

The cytotoxicity assay results are expressed as mean ± standard deviation (SD). Intergroup differences were evaluated using one-way ANOVA, followed by pairwise comparisons with paired t-tests and LSD tests. All statistical analyses were performed using SPSS version 20, and p-values < 0.05 were considered statistically significant [43].

In this study, uppercase and lowercase letters in data tables are used to distinguish statistical groups and significance levels. Identical letters denote no statistically significant difference, whereas different letters indicate significant differences. Specifically, capital letters are used to compare means across columns, while lowercase letters compare rows. This methodology provides a clear and efficient way to present complex statistical data, facilitating rapid interpretation by readers without the need for elaborate explanations.

3. RESULTS

3.1. Cytotoxic assay

3.1.1. Cytotoxic Efficacy and Selectivity of the Albendazole-Etoricoxib Mixture

The cytotoxic efficacy of the Albendazole-Etoricoxib combination was quantitatively evaluated against HeLa (cervical carcinoma) and HFF (human foreskin fibroblast) cell lines employing the MTT assay at exposure durations of 24 and 72 hours. The findings, as summarized in Tables **1** and **2**, indicate a concentration- and time-dependent suppression of cellular proliferation, exhibiting notable selectivity for the cancerous cell line.

In HeLa cells, the mixture demonstrated significant anti-proliferative activity. Following a 24-hour treatment period, percent inhibition ranged from 11.8 ± 1.2% at the lowest concentration (0.1 µg/mL) to 66.5 ± 2.4% at the highest concentration (1,000 µg/mL). Efficacy was markedly enhanced after 72 hours of incubation, with inhibition increasing to 24.8 ± 1.2% at 0.1 µg/mL and 86.8 ± 1.9% at 1,000 µg/mL. This time-dependent increase in cytotoxicity was statistically significant ($p < 0.05$) across all concentrations tested. The IC_{50} value of the mixture against HeLa cells decreased considerably from 150 µg/mL at 24 hours to 87.5 µg/mL at 72 hours, further corroborating the observed increase in potency with extended exposure (Table **1**).

In contrast to the cancerous cell lines, the HFF non-cancerous cell line exhibited substantial resistance to the drug mixture. The maximum inhibition recorded in HFF cells was merely 9.7 ± 1.8% at 24 hours and 12.8 ± 1.5% at 72 hours, even when exposed to the highest concentration of 1,000 µg/mL. Inhibition rates at lower concentrations were minimal or negligible. As a result, the IC_{50} value for HFF cells remained above 1,000 µg/mL at both time points, signifying very low inherent cytotoxicity (Table **2**).

The direct statistical comparison of effects on the two cell lines, as presented in Table **2**, showed that proliferation inhibition was significantly more pronounced in HeLa cells than in HFF cells across all concentrations and time points. This marked differential cytotoxicity highlights a favorable selective index for the Albendazole-Etoricoxib combination, indicating its preferential targeting of malignant cells while minimizing effects on normal fibroblasts.

3.1.2. Cytotoxicity of 5-Fluorouracil

The cytotoxicity of 5-Fluorouracil (5-FU) was assessed in both HeLa and HFF cell lines to facilitate

Table 1: The Effect of the Mixture on the Survival of HeLa and HFF Cell Lines at 24 and 72 Hours

Con. (µg/ml)	Cellular proliferation inhibition (mean ± SD)					
	HeLa cell line			HFF cell line		
	24 hr.	72 hr.	*P*- value	24 hr.	72 hr.	*P*- value
0.1	E 11.8 ± 1.2	E 24.8 ± 1.2	<0.001*	B 0.0 ± 0.0	E 0.0 ± 0.0	N. S
1	D 23.8 ± 1.5	D 38.3 ± 1.6	<0.001*	B 0.2 ± 0.4	D 1.2 ± 0.8	0.017
10	C 32.7 ± 1.8	C 42.8 ± 1.5	<0.001*	B 2.0 ± 0.9	C 5.0 ± 0.9	<0.001
100	B 46.8 ± 2.0	B 50.7 ± 1.6	0.003*	A 7.3 ± 1.2	B 9.2 ± 1.2	0.005
1000	A 66.5 ± 2.4	A 86.8 ± 1.9	<0.001*	A 9.7 ± 1.8	A 12.8 ± 1.5	<0.001
IC 50	150 µg/ml	87.5 µg/ml	-	>1000 µg/ml	>1000 µg/ml	-
LSD value	4.28	3.78	-	2.44	2.42	-
*: indicates p < 0.05.						

Table 2: Comparison of the Cytotoxic Effects of the Mixture on HeLa and HFF Cells

Con. (µg/ml)	Cellular proliferation inhibition (mean ± SD)					
	24 hr.			72 hr.		
	HeLa cell line	HFF cell line	*P*- value	HeLa cell line	HFF cell line	*P*- value
0.1	E 11.8 ± 1.2	B 0.0 ± 0.0	<0.001*	E 24.8 ± 1.2	E 0.0 ± 0.0	<0.001*
1	D 23.8 ± 1.5	B 0.2 ± 0.4	<0.001*	D 38.3 ± 1.6	D 1.2 ± 0.8	<0.001*
10	C 32.7 ± 1.8	B 2.0 ± 0.9	<0.001*	C 42.8 ± 1.5	C 5.0 ± 0.9	<0.001*
100	B 46.8 ± 2.0	A 7.3 ± 1.2	<0.001*	B 50.7 ± 1.6	B 9.2 ± 1.2	<0.001*
1000	A 66.5 ± 2.4	A 9.7 ± 1.8	<0.001*	A 86.8 ± 1.9	A 12.8 ± 1.5	<0.001*
IC 50	150 µg/ml	>1000 µg/ml	-	87.5 µg/ml	>1000 µg/ml	-
LSD value	4.28	2.44	-	3.78	2.42	-
*: indicates p < 0.05.						

comparison. The findings demonstrated a distinct cytotoxic profile compared with the Albendazole-Etoricoxib combination (Table **3**).

This study demonstrated that 5-fluorouracil (5-FU) exerted a concentration-dependent inhibitory effect on both cell lines. Specifically, in HeLa cells, proliferation decreased from 4.2 ± 0.8% at 0.1 µg/mL to 59.8 ± 2.4% at 1,000 µg/mL after 24 hours of treatment. Notably, after 72 hours of exposure, the inhibitory effect on HeLa cells was generally attenuated at higher concentrations, with the reduction in proliferation decreasing to 46.5 ± 2.4% at 1,000 µg/mL. This temporal decline in efficacy was statistically significant ($p < 0.05$) at concentrations of 1 µg/mL or higher. The calculated IC_{50} values for HeLa cells were 365.7 µg/mL at 24 hours and exceeded 1,000 µg/mL at 72 hours, indicating a reduction in sensitivity over time.

In contrast, 5-FU exhibited a more potent and time-dependent cytotoxic effect on the non-malignant HFF cell line. Inhibition rates in HFF cells increased from 2.8 ± 1.2% at 24 hours to 10.7 ± 1.2% at 72 hours at a concentration of 0.1 µg/mL, consistent across all tested concentrations. At the highest concentration tested (1,000 µg/mL), inhibition significantly increased from 54.5 ± 3.8% at 24 hours to 72.0 ± 2.8% at 72 hours ($p < 0.001$). The half-maximal inhibitory concentration (IC_{50}) for HFF cells markedly decreased from 370.1 µg/mL at 24 hours to 50.2 µg/mL at 72 hours, reflecting a pronounced increase in cytotoxicity towards normal fibroblasts over time.

A comparative analysis of the two cell lines reveals a significant finding: after 72 hours of exposure, 5-fluorouracil (5-FU) showed greater cytotoxicity against normal HFF cells (IC_{50} = 50.2 µg/mL) than against HeLa cancer cells (IC_{50}> 1,000 µg/mL). This observation suggests the absence of selective cytotoxicity under the experimental conditions, as normal cells were more adversely affected than targeted cancer cells after extended treatment.

3.1.3. Cytotoxicity of Individual Mixture Medications

The study comprehensively examines the cytotoxic effects of Albendazole and Etoricoxib to elucidate their combined mechanisms of toxicity. Additionally, it evaluates the nature of their interaction to determine whether their effects are synergistic, antagonistic, or additive.

3.1.3.1. Albendazole Cytotoxicity

The cytotoxicity of Albendazole on HeLa cells was assessed at 24 and 72 hours. Results demonstrated a concentration- and time-dependent inhibition of cell proliferation. At 24 hours, the maximum inhibition observed was 40.8 ± 2.4% at 1000 µg/mL, indicating a modest effect. In contrast, after 72 hours, the anti-proliferative activity was markedly enhanced, reaching 52.7 ± 2.5% at the highest concentration. Additionally, the IC_{50} value decreased significantly from greater than 1000 µg/mL at 24 hours to 702.3 µg/mL at 72 hours, further confirming the increased efficacy of Albendazole with prolonged exposure against cervical cancer cells (see Table **4**).

3.1.3.2. Etoricoxib Cytotoxicity

The antiproliferative effects of Etoricoxib on HeLa cells were evaluated, demonstrating concentration-dependent inhibition of cell proliferation at both 24 and 72 hours. The inhibitory effect was notably amplified over time at concentrations up to 10 µg/mL. However, the efficacy plateaued at higher concentrations, with 100 µg/mL and 1000 µg/mL exhibiting comparable potency. Accordingly, the IC_{50} value remained above 1000 µg/mL at both time points. These findings suggest that although Etoricoxib exerts a statistically

Table 3: The Impact of 5-FU on Survival Rates of HeLa and HFF Cell Lines at 24 and 72 hours

Con. (µg/ml)	Cellular proliferation inhibition (mean ± SD)					
	HeLa cell line			HFF cell line		
	24 hr.	72 hr.	*P*- value	24 hr.	72 hr.	*P*- value
0.1	E 4.2 ± 0.8	E 3.2 ± 0.8	0.056	E 2.8 ± 1.2	E 10.7 ± 1.2	<0.001*
1	D 16.0 ± 1.4	D 9.8 ± 1.2	<0.001*	D 16.5 ± 1.9	D 24.7 ± 2.1	<0.001*
10	C 23.7 ± 1.8	C 20.8 ± 1.5	0.009*	C 25.8 ± 2.7	C 40.8 ± 2.1	<0.001*
100	B 43.5 ± 2.3	B 32.7 ± 1.9	<0.001*	B 46.2 ± 3.3	B 58.5 ± 2.4	<0.001*
1000	A 59.8 ± 2.4	A 46.5 ± 2.4	<0.001*	A 54.5 ± 3.8	A 72.0 ± 2.8	<0.001*
IC 50	365.7 µg/ml	>1000 µg/ml		370.1 µg/ml	50.2 µg/ml	-
LSD value	4.32	3.85		6.34	5.32	-
*: significant at (P<0.05)						

Table 4: The Effect of Albendazole on the Survival Rates of Cervical Cancer Cells at 24 and 72 hours

Concentration (µg/ml)	Cellular proliferation inhibition (mean ± SD)		*P*- value
	24 hr.	72 hr.	
0.1	E 0 ± 0.00	E 4.0 ± 0.9	<0.001*
1	D 8.8 ± 1.2	D 12.3 ± 1.6	0.002*
10	C 12.0 ± 1.4	C 26.8 ± 1.5	<0.001*
100	B 32.5 ± 1.9	B 42.8 ± 1.5	<0.001*
1000	A 40.8 ± 2.4	A 52.7 ± 2.5	<0.001*
IC 50	>1000 µg/ml	702.3 µg/ml	-
LSD value	3.92	4.1	-
*: significant at (P<0.05)			

significant cytotoxic effect on HeLa cells, its monotherapy potency appears limited.

3.1.4. Comparison of Cytotoxicity among Albendazole, Etoricoxib,5-FU, and the Mixture

The anti-proliferative activity of Albendazole, Etoricoxib, 5-FU, and their combination was evaluated against HeLa cells over 24 and 72 hours. Results indicated that after 24 hours, the drug combination exhibited the highest potency, with 66.5% inhibition at 1000 µg/mL. The IC_{50} value for the combination was 150 µg/mL, markedly lower than that of 5-FU (365.7 µg/mL) and the individual agents, which all exhibited IC_{50} values exceeding 1000 µg/mL (Tables **6** and **7**).

This enhanced effect was more evident following 72 hours of exposure. The mixture achieved a remarkable 86.8% inhibition at the highest concentration, significantly surpassing the maximal effect observed with any single agent. Correspondingly, its IC_{50} value decreased to 87.5 µg/mL, whereas the individual agents, with Albendazole being the most potent (IC_{50} = 702.3 µg/mL), demonstrated substantially lower efficacy. Across all tested concentrations and time points, the combination consistently yielded the highest growth inhibition, indicating a markedly synergistic cytotoxic response relative to monotherapies (Tables **6** & **7**).

3.2. Selective Toxicity Assay

The study demonstrated an increase in the selectivity index (SI) of the Albendazole–Etoricoxib mixture, from 6.66 at 24 hours to 11.42 at 72 hours, indicating enhanced targeted efficacy against cancer cells over time. Conversely, the SI for 5-fluorouracil (5-FU) declined significantly, from 1.01 at 24 hours to 0.050 at 72 hours, suggesting diminished specificity for cancer cell targeting with extended exposure. This reduction may be attributed to the development of resistance mechanisms by cancer cells in response to prolonged 5-FU treatment (Table **8**).

3.3. Synergistic Anticancer Effects of the Etoricoxib and Albendazole Combination

The combined anticancer effects of Etoricoxib and Albendazole were tested *in vitro*, demonstrating concentration-dependent synergism, as determined using the Chou-Talalay method with Compusyn software. The key Combination Index (CI) and Dose

Table 5: The Effect of Etoricoxib on the Survival Rates of Cervical Cancer Cells after 24 and 72 hours

Concentration (µg/ml)	Cellular proliferation inhibition (mean ± SD)		*P*- value
	24 hr.	72 hr.	
0.1	C 1.0 ± 0.8	D 3.0 ± 0.9	0.001
1	C 3.8 ± 1.2	D 6.8 ± 1.2	0.001
10	B 21.7 ± 2.2	C 29.7 ± 2.1	<0.001
100	A 41.7 ± 2.2	B 40.7 ± 2.1	0.441
1000	A 42.8 ± 2.4	A 47.5 ± 2.7	0.013
IC 50	>1000 µg/ml	>1000 µg/ml	-
[b] LSD value	4.46	4.73	-
*: indicates p < 0.05.			

Table 6: Comparison of Albendazole, Etoricoxib, 5-FU, and the Mixture for Inhibiting the Growth of HeLa Cancer Cells over 24 hours

Concentration (µg/ml)	Cellular proliferation inhibition (mean ± SD)				LSD
	Albendazole	Etoricoxib	5-FU	mix	
0.1	E 0 ± 0.00	C 1.0 ± 0.8	E 4.2 ± 0.8	E 11.8 ± 1.2	2.14
1	D 8.8 ± 1.2	C 3.8 ± 1.2	D 16.0 ± 1.4	D 23.8 ± 1.5	3.17
10	C 12.0 ± 1.4	B 21.7 ± 2.2	C 23.7 ± 1.8	C 32.7 ± 1.8	4.24
100	B 32.5 ± 1.9	A 41.7 ± 2.2	B 43.5 ± 2.3	B 46.8 ± 2.0	4.97
1000	A 40.8 ± 2.4	A 42.8 ± 2.4	A 59.8 ± 2.4	A 66.5 ± 2.4	5.94
IC 50	>1000 µg/ml	>1000 µg/ml	365.7 µg/ml	150 µg/ml	-
LSD value	3.92	4.46	4.32	4.28	-
*: indicates p < 0.05.					

Table 7: Comparison of Albendazole, Etoricoxib, 5-FU, and the Mixture for Inhibiting the Growth of HeLa Cancer Cells over 72 hours

Concentration (µg/ml)	Cellular proliferation inhibition (mean ± SD)				[b]LSD value
	Albendazole	Etoricoxib	5-FU	mix	
0.1	E 4.0 ± 0.9	D 3.0 ± 0.9	E 3.2 ± 0.8	E 24.8 ± 1.2	2.27
1	D 12.3 ± 1.6	D 6.8 ± 1.2	D 9.8 ± 1.2	D 38.3 ± 1.6	3.42
10	C 26.8 ± 1.5	C 29.7 ± 2.1	C 20.8 ± 1.5	C 42.8 ± 1.5	4.03
100	B 42.8 ± 1.5	B 40.7 ± 2.1	B 32.7 ± 1.9	B 50.7 ± 1.6	4.26
1000	A 52.7 ± 2.5	A 47.5 ± 2.7	A 46.5 ± 2.4	A 86.8 ± 1.9	6.03
IC 50	702.3 µg/ml	>1000 µg/ml	>1000 µg/ml	87.5 µg/ml	-
LSD value	4.1	4.73	3.85	3.78	-
*: indicates p < 0.05.					

Reduction Index (DRI) values for a 1:1 molar ratio at 24 and 72 hours are shown in Table **9**.

At 24 hours, the combination exhibited strong synergism (CI < 0.1) at lower concentrations (0.1–10 µg/mL total mixture), with CI values ranging from 0.00736 to 0.07892. This synergistic effect diminished at higher concentrations, with a CI of 0.30776 at 100 µg/mL, and approached additivity (CI = 0.92533) at 1000 µg/mL. DRI values across the concentration range remained significantly above 1, indicating a substantial potential for dose reduction when both drugs are used together Table **9**, Figure **2**.

This synergistic profile was further enhanced and sustained over an extended period. After 72-hour incubation, the combination maintained Very Strong Synergism across most concentrations, including the highest concentration of 1000 µg/ml (CI = 0.01651), at which the effect was nearly additive at 24 hours. A transition to Strong Synergism was observed only at the 100 µg/ml concentration (CI = 0.23860). Notably, the Drug Reduction Index (DRI) values remained significantly high after 72 hours, particularly at the lowest concentration (0.1 µg/ml), where values exceeded 300 for Albendazole and 500 for Etoricoxib.

Table 8: Selective Toxicity Index (SI) of the Albendazole-Etoricoxib Mixture and 5-FU

Treatment Group	Incubation Time	IC_{50} (HeLa)	IC_{50} (HFF)	Selective Toxicity Index (SI)
Mixture	24 hours	150 µg/mL	>1000 µg/mL	6.66
	72 hours	87.5 µg/mL	>1000 µg/mL	>11.42
5-FU	24 hours	365.7 µg/mL	370.1 µg/mL	1.01
	72 hours	>1000 µg/mL	50.2 µg/mL	0.050

The Selective Toxicity Index (SI) was calculated as SI = IC_{50} of normal HFF cells / IC_{50} of cancerous HeLa cells. An SI > 1 indicates preferential cytotoxicity toward cancer cells. The IC_{50} values were derived from MTT assays after 24 and 72 hours of incubation.

Table 9: Mixtures CI and DRI following 24 and 72 Hours of Incubation

24-hour incubation period						
DRI value		Combination pattern	CI score	(concentration µg/ml) The ratio of Albendazole, etoricoxib in the combination is 1:1		
Etoricoxib	Albendazole			Etoricoxib	Albendazole	mixture
175.773*	598.040*	Very Strong Synergism	0.00736	0.05	0.05	0.1
95.8909*	164.588*	Very Strong Synergism	0.01650	0.5	0.5	1
23.2173*	27.8968*	Very Strong Synergism	0.07892	5	5	10
7.61555*	5.66747*	Synergism	0.30776	50	50	100
3.88132*	1.49771*	Nearly Additive	0.92533	500	500	1000
72-hour incubation period						
525.205*	308.166*	Very Strong Synergism	0.00515	0.05	0.05	0.1
265.208*	180.548*	Very Strong Synergism	0.00931	0.5	0.5	1
42.7871*	30.4359*	Very Strong Synergism	0.05623	5	5	10
9.65879*	7.40376*	Strong Synergism	0.23860	50	50	100
111.676*	132.389*	Very Strong Synergism	0.01651	500	500	1000

Compusyn software was used to calculate the Combination Index (CI) and Dose Reduction Index (DRI) values. A CI above 1 signifies antagonism, a CI of exactly 1 indicates an additive effect, and a CI below 1 suggests synergy. A DRI greater than 1 reflects decreased toxicity. An asterisk (*) marks a beneficial reduction in the effective cytotoxic concentration [44].

This underscores a substantial dose-reduction advantage and a decreased risk of toxicity with prolonged exposure. Collectively, these findings suggest that the combination of Etoricoxib and Albendazole is highly synergistic and therapeutically advantageous, capable of eliciting potent cytotoxic effects at markedly reduced concentrations of each agent Table **9**, Figure **1**.

3.6. Lactate Production Assessment

To clarify the individual and combined effects of Albendazole and Etoricoxib on cancer cell metabolism (cellular glycolytic rate), we measured extracellular lactate levels—a direct indicator of glycolytic activity—in HeLa and HFF cell lines after 24 hours of treatment. The results demonstrate both specific and synergistic anti-glycolytic effects.

As a single agent, Etoricoxib caused a moderate, concentration-dependent decrease in lactate production in HeLa cells, reaching maximum inhibition at 1000 µg/mL (reducing from 12.1 to 7.0 nmol/mg protein). In contrast, albendazole monotherapy produced a greater, dose-dependent reduction in lactate levels at the same concentration. Notably, combining Albendazole with Etoricoxib resulted in a strongly synergistic suppression of glycolysis. At 1000 µg/mL, the combination lowered lactate production to 1.8 nmol/mg protein, a level significantly lower than with either drug alone. Additionally, the IC_{50} values for glycolytic inhibition highlight this synergy, with the combination (45.2 µg/mL) demonstrating greater potency than albendazole (185.5 µg/mL) or Etoricoxib (IC_{50}> 1000 µg/mL).

This study shows that the anti-metabolic effect was definite to cancer cells. In the non-cancerous HFF cell

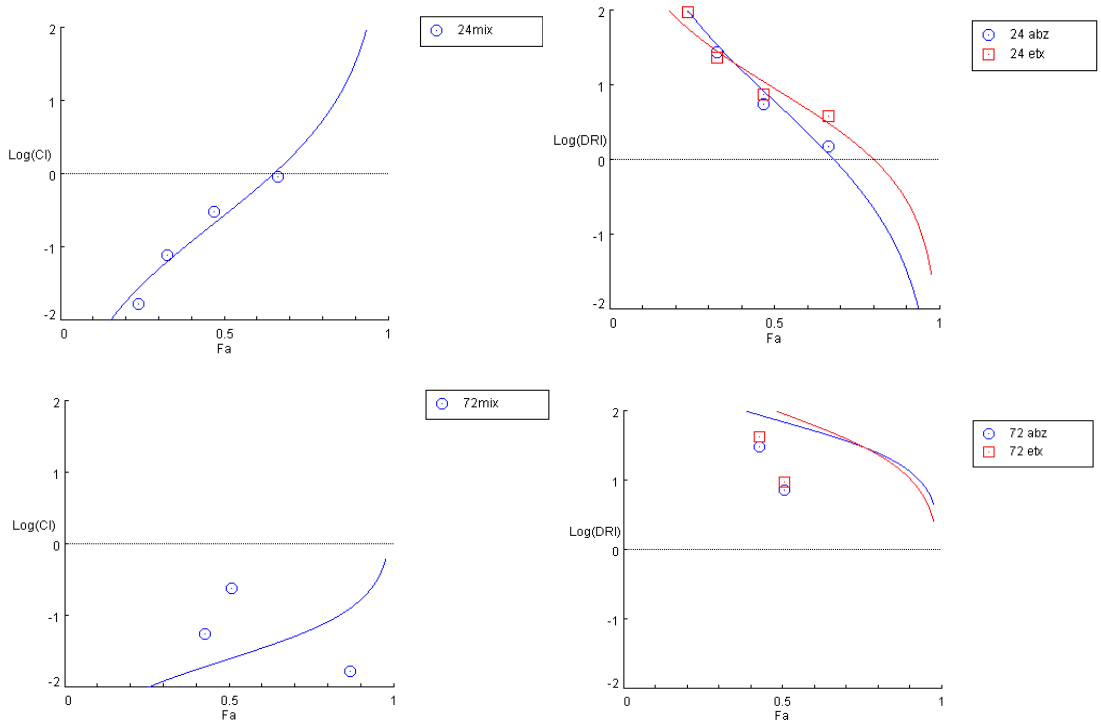

Figure 1: The logarithm of the combination index (CI) on the left and the logarithm of the dose reduction index (DRI) on the right for the mixture observed at 24 hours (top panel) and 72 hours (bottom panel) of incubation. etx: Etoricoxib, abz: Albendazole, CI: combination index, and DRI: dose reduction index.

Table 10: Effect of Albendazole, Etoricoxib, and their Mixture on Lactate Production in HeLa and HFF Cell Lines after 24 Hours

Concentration (µg/mL)	Treatment	Lactate Production (nmol/mg protein, Mean ± SD)		P-value (HeLa vs. HFF)
		HeLa cell line	HFF cell line	
0 (Control)	-	A12.1 ± 0.8 a	A12.1 ± 0.7 a	1.000
100	Albendazole	C 6.2 ± 0.4 b	A 11.6 ± 0.5 a	<0.001*
	Etoricoxib	B 8.5 ± 0.6 b	A 11.8 ± 0.6 a	<0.001*
	Mixture	E 2.7 ± 0.2 b	B 11.0 ± 0.6 a	<0.001*
1000	Albendazole	D 5.0 ± 0.3 b	A 11.2 ± 0.6 a	<0.001*
	Etoricoxib	C 7.0 ± 0.5 b	A 11.5 ± 0.7 a	<0.001*
	Mixture	E 1.8 ± 0.2 b	C 10.2 ± 0.6 a	<0.001*
IC_{50} (Glycolysis)	Albendazole	>1000 µg/mL	>1000 µg/mL	-
	Etoricoxib	185.5 µg/mL	>1000 µg/mL	-
	Mixture	45.2 µg/mL	>1000 µg/mL	-
LSD value		0.95	1.02	

Data are presented as mean ± standard deviation (SD), with a sample size of six (n = 6). Within each treatment group, different uppercase superscripts (A, B, C) indicate significant differences among concentrations. Conversely, within each row, different lowercase superscript letters (a, b, c, d) denote significant differences among treatments at the same concentration. Statistical significance was determined using one-way ANOVA followed by the least significant difference (LSD) post-hoc test; letters represent p-values less than 0.05. The p-value in the final column reflects the significance of differences between the two cell lines for each treatment and concentration, assessed via a paired t-test. An asterisk (*) indicates a p-value less than 0.05.

line, treatments did not cause a significant drop in lactate production at concentrations below 100 µg/mL. At the highest concentration tested, only a slight decrease was observed in the mixture, whereas the cells largely maintained baseline glycolytic activity when exposed to the individual drugs Table **10**.

3.7. Esterase Activity Assay

To clarify the individual and combined effects of Albendazole and Etoricoxib on cellular pH regulatory mechanisms, the esterase activity of Carbonic Anhydrase (CA) in cell lysates was evaluated. It was

shown that etoricoxib was the main agent responsible for CA inhibition. This inhibitory effect was notably increased when etoricoxib was used in combination therapy.

Monotherapy with Albendazole produced only a modest, non-statistically significant decrease in carbonic anhydrase (CA) activity in HeLa cells, even at the highest concentrations tested. In contrast, Etoricoxib monotherapy showed an apparent, concentration-dependent inhibition, reducing CA activity at 1000 µg/mL. Notably, the combination of Albendazole and Etoricoxib produced the most significant effect, with CA activity decreased at 1000 µg/mL—a reduction that was significantly greater than with Etoricoxib alone. The IC_{50} for CA inhibition by the combination was 38.7 µg/mL, indicating greater potency than Etoricoxib monotherapy (IC_{50} = 205.8 µg/mL).

This targeted disruption of pH regulation was uniquely specific to cancer cells. In HFF cells, carbonic anhydrase (CA) activity remained mostly unaffected across all treatment groups. The minor reductions observed at the highest mixture concentration were negligible relative to the significant inhibition in HeLa cells, indicating a favorable therapeutic window. These results are further supported by molecular docking data, which show specific binding of Etoricoxib to the cancer-associated CA-IX isoform Table **11**.

3.5. Molecular Docking Studies

Molecular docking simulations were conducted to investigate the interactions of Albendazole and etoricoxib with key components of the "Growth Hub" and "Power Hub.' represented by the human wild-type β-tubulin subunit (PDB ID: 5C8Y) and Carbonic Anhydrase IX (CA-IX) (PDB ID: 5DVX). The selection of these targets was based on their structural stability and relevance to disease pathology, rendering them potential candidates for cancer therapeutic strategies. The analyses were performed using established computational tools, including AutoDock Tools 1.5.7, BIOVIA Discovery Studio, UCSF Chimera, and AutoDock [45].

3.5.1. Docking with β-tubulin Subunit

The molecular docking analysis indicated that Albendazole interacts with the human wild-type β -tubulin subunit, yielding a docking score of -6.7 kcal/mol. The interaction profile includes two conventional hydrogen bonds: one with ASN A:206 at a distance of 2.80 Å and another with TYR A:224 at 2.35 Å. Additionally, a single-carbon hydrogen bond was identified between GLU A:183 and a water molecule at 3.39 Å. An alkyl bond was observed with ALA A:99 at 5.30 Å, and a pi-alkyl interaction occurs with ALA A:12 at 4.83 Å (see Figure **3**).

For comparison, a molecular docking study was conducted using Plinabulin, a β-tubulin inhibito [46],

Table 11: Effect of Albendazole, Etoricoxib, and their Mixture on Carbonic Anhydrase Esterase Activity in HeLa and HFF Cell Lines after 24 Hours

Concentration (µg/mL)	Treatment	Carbonic Anhydrase Activity (ΔA/min/mg protein, Mean ± SD)		P-value (HeLa vs. HFF)
		HeLa cell line	HFF cell line	
0 (Control)	-	A15.3 ± 0.9 a	A15.3 ± 0.8 a	1.000
100	Albendazole	A14.2 ± 0.8 a	A15.0 ± 0.9 a	0.112
	Etoricoxib	B8.1 ± 0.5 b	A14.7 ± 0.7 a	<0.001*
	Mixture	D3.2 ± 0.3b	AB14.3 ± 0.7 a	<0.001*
1000	Albendazole	A13.8 ± 0.9 a	A14.9 ± 0.8 a	0.058
	Etoricoxib	C6.1 ± 0.4 b	AB14.5 ± 0.8 a	<0.001*
	Mixture	D2.1 ± 0.3 b	B13.4 ± 0.8a	<0.001*
IC_{50} (Glycolysis)	Albendazole	>1000 µg/mL	>1000 µg/mL	-
	Etoricoxib	205.8 µg/mL	>1000 µg/mL	-
	Mixture	38.7 µg/mL	>1000 µg/mL	-
LSD value		1.11	1.18	

Data are expressed as mean ± standard deviation (SD) with a sample size of six (n=6). Within each treatment group, different uppercase superscripts (A, B, C) indicate significant differences among concentrations. Within each row, different lowercase superscript letters (a, b, c) denote significant differences between treatments at the same concentration. Statistically significant differences ($p < 0.05$) were identified using one-way ANOVA followed by LSD post-hoc tests. The P-value presented in the final column reflects the significance of differences between the two cell lines for each treatment and concentration, as assessed by a paired t-test. An asterisk (*) indicates a p-value less than 0.05.

with the human wild-type β-tubulin subunit, which yielded a docking score of -8.2 kcal/mol. The interaction profile reveals two conventional hydrogen bonds: one with ALA A:12 at 2.79 Å and another with ASN A:101 at 2.73 Å. Additionally, a two-carbon

hydrogen bond was observed with two ASP A:69 residues at 3.78 Å and 3.69 Å. A pi-anion interaction was identified with GLU A:183 at 3.76 Å, along with a pi-alkyl interaction involving ALA A:12 at 4.93 Å (see Figure **2**).

3.5.2. Docking with Carbonic Anhydrase IX (CA-IX)

The molecular docking analysis between Carbonic Anhydrase IX and etoricoxib showed a binding affinity of -7.1 kcal/mol. The interaction interface included four conventional hydrogen bonds: two with ARG A:196 at 2.22 Å and 2.31 Å, one with ASN A:198 at 2.02 Å, and one with THR A:333 at 2.98 Å. Additionally, a carbon-hydrogen bond was observed with ARG A:196 at 3.67 Å, along with a pi-donor hydrogen bond with THR A:333 at 2.68 Å. Other interactions consisted of a pi-sigma bond with HIS A:226 at 3.75 Å, a pi-pi T-shaped interaction with HIS A:226 at 5.12 Å, and an alkyl bond with PRO A:335 at 4.47 Å (Figure **4**).

In a comparative analysis, molecular docking was performed for Slc-0111, a carbonic anhydrase inhibitor [47], against carbonic anhydrase IX. The docking score was -7.4 kcal/mol. The interaction profile showed three conventional hydrogen bonds: one with GLY A:144 at 1.91 Å, another with TRP A:149 at 2.48 Å, and a third with GLY A:145 at 2.18 Å. Additionally, a hydrogen bond was observed with TYR A:143 at 3.71 Å. The study also identified pi-pi stacking interactions involving TRP A:149 residues at 3.75 Å and 3.90 Å, as well as pi-alkyl interactions with ARG A:376 at 5.39 Å and ALA A:157 at 5.13 Å (Figure **3**).

3.5.3. Comparative Analysis of Molecular Docking with Reference Inhibitors

Molecular docking analyses were conducted to compare the binding of Albendazole and Etoricoxib with those of standard inhibitors at their respective targets. Albendazole exhibited a binding affinity for the β-tubulin subunit (PDB ID: 5C8Y) with a docking score of -6.7 kcal/mol. Its interaction was characterized by the formation of conventional hydrogen bonds with ASN A:206 and TYR A:224, along with hydrophobic contacts involving ALA A:12 and ALA A:99. In comparison, the reference β -tubulin inhibitor, Plinabulin, demonstrated a higher affinity of -8.2

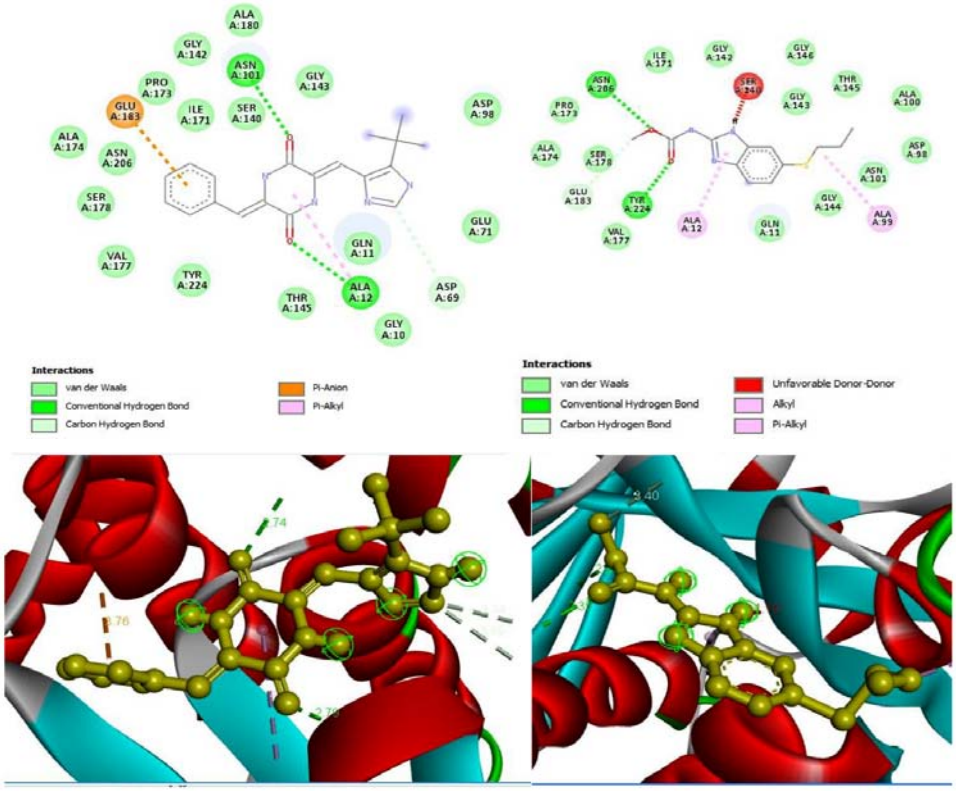

Figure 2: The structural configurations of the human wild-type β -tubulin subunit binding sites are depicted in both two-dimensional (upper image) and three-dimensional (lower image) views, illustrating the binding sites of albendazole (right image) and Plinabulin (left image) on the β-tubulin subunit.

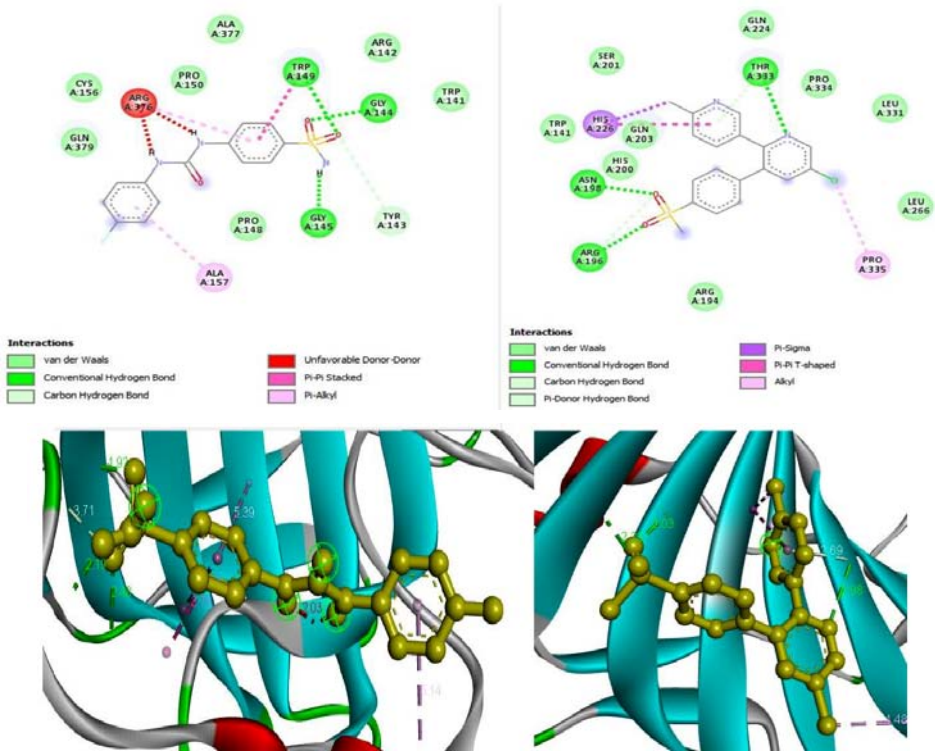

Figure 3: The structural configurations of the Carbonic Anhydrase IX binding sites are shown in both two-dimensional (upper image) and three-dimensional (lower image) views, depicting the binding sites of etoricoxib (right image) and Slc-0111 (left image) on the Carbonic Anhydrase enzyme.

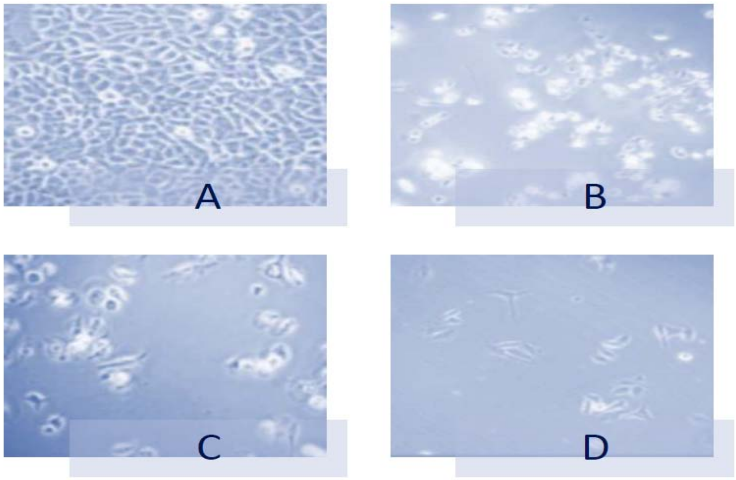

Figure 4: The morphological features of HeLa cells were observed under an inverted microscope. (**A**) Untreated HeLa cells acted as controls. (**B**) HeLa cells were treated with 100 µg/mL of Etoricoxib for 72 hours. (**C**) HeLa cells were exposed to 1,000 µg/mL of Albendazole for 72 hours. (**D**) HeLa cells were also treated with a 1,000 µg/mL mixture for the same duration.

kcal/mol, establishing hydrogen bonds with ALA A:12 and ASN A:101, as well as a significant pi-anion interaction with GLU A:183, supplemented by additional stabilizing interactions.

For the targeted Carbonic Anhydrase IX (CA-IX; PDB ID: 5DVX), Etoricoxib exhibited a binding affinity of -7.1 kcal/mol. The compound interacted with the active site through multiple hydrogen bonds involving residues ARG A:196, ASN A:198, and THR A:333, as well as pi-interactions with HIS A:226. The established CA-IX inhibitor SLC-0111 demonstrated a slightly superior binding score of -7.4 kcal/mol, mediated by hydrogen bonds with residues GLY A:144, TRP A:149, and GLY A:145, and stabilized by pi-pi stacking interactions with TRP A:149.

Overall, although the conventional inhibitors Plinabulin and SLC-0111 exhibited marginally superior

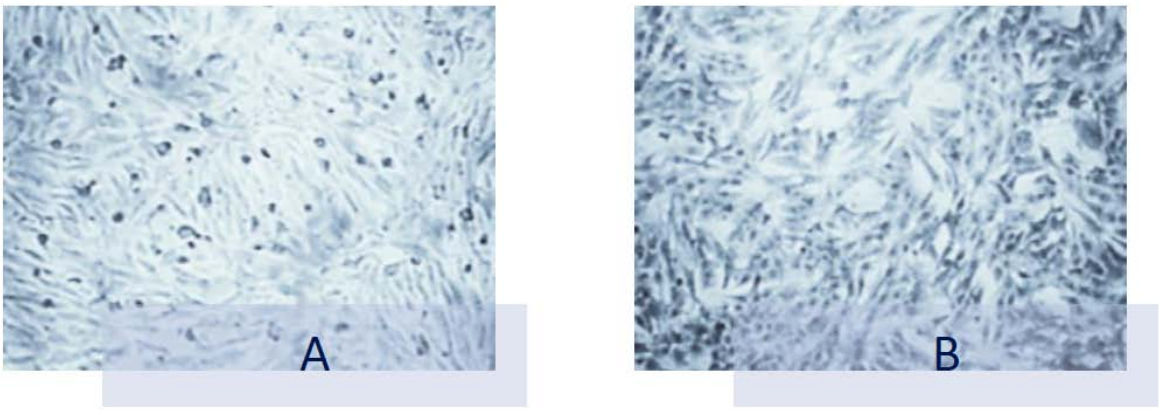

Figure 5: Morphological features of human foreskin fibroblast cells (HFF) were observed under an inverted microscope. (**A**) Untreated HFF cell line. (**B**) HFF cells were treated with a 1000 µg/ml mixture for 72 hours.

binding affinities and more complex interaction profiles, both Albendazole and Etoricoxib demonstrated notable and specific binding to their respective targets. This observation offers a credible structural basis for their biological activities and underscores their potential utility in synergistic anti-cancer regimens.

3.6. Morphological Assessment of Cytotoxicity

The cytotoxic effects of Etoricoxib, Albendazole, and their combination on HeLa cervical cancer cells and non-cancerous human foreskin fibroblast (HFF) cells were further assessed by examining morphological changes under an inverted microscope following the MTT assay.

In HeLa cells (Figure **5A-5D**), the untreated controls exhibited a characteristic epithelial-like morphology, characterized by adherence, widespread spreading, and a densely packed cobblestone appearance (Figure **5A**). Treatment with 100 µg/mL of Etoricoxib for 72 hours induced notable cytotoxic effects (Figure **5B**), including a decrease in cell density and a shift towards a rounded, shrunken morphology indicative of apoptosis. Additionally, a significant number of cells detached from the culture surface, leaving observable gaps in the monolayer.

Exposure to a high concentration of Albendazole (1,000 µg/mL) for 72 hours induced significant morphological alterations (see Figure **5C**). The HeLa cell monolayer showed considerable disruption, with numerous cells detaching or losing adherence. Remaining adherent cells displayed pronounced shrinkage, membrane blebbing, and a loss of their characteristic polygonal morphology. The combined treatment with both drugs at the same concentration (Figure **5D**) yielded effects comparable to Albendazole alone, characterized by extensive cell detachment and morphological abnormalities, indicative of pronounced cytotoxicity.

The non-cancerous HFF cell line exhibited significant resistance to the drug treatment under identical conditions. Untreated HFF control cells (Figure **5A**) displayed the characteristic elongated, spindle-shaped morphology typical of healthy fibroblasts, forming a confluent and organized monolayer. Notably, after 72 hours of exposure to the high-concentration drug mixture (1,000 µg/mL), the HFF cells (Figure **5B**) maintained their fibroblastic morphology and adhesion properties. Although a slight reduction in overall confluency was occasionally observed, the cells largely remained intact and spread, with no evident signs of severe cytotoxicity, unlike in the HeLa cell line (Figures **4,5**).

4. DISCUSSION

Managing advanced cervical cancer remains a major clinical challenge, mainly because of the toxicities linked to standard chemotherapies and the frequent development of chemoresistance. This highlights an urgent need for innovative treatments that are both effective and selective. Drug repurposing offers a promising path to implement these strategies quickly. The current study aims to fill a critical knowledge gap: the largely unexplored potential of combining Albendazole, a microtubule-disrupting anthelmintic, with Etoricoxib, a COX-2 inhibitor, to achieve synergistic cytotoxicity against cervical cancer. We hypothesize that this combination could disrupt glycolytic metabolism and cellular pH regulation in cancer cells by simultaneously targeting structural integrity and metabolic pathways, which we term (Energetic Strangulation).

Our findings robustly confirm this hypothesis. The results demonstrate that the combination of Albendazole and Etoricoxib exhibits potent, synergistic cytotoxic effects against HeLa cervical cancer cells, significantly surpassing the efficacy of either agent alone or the standard chemotherapeutic agent 5-FU. This synergy was quantified using a Combination Index (CI) below one and a favorable Dose Reduction Index (DRI), suggesting that lower, potentially safer doses of each drug could be used effectively. Importantly, this combination showed remarkable selectivity for malignant cells, sparing non-malignant human foreskin fibroblasts (HFF), whereas 5-FU exhibited increased toxicity toward normal cells over time. Mechanistic studies indicated that the combination markedly suppressed glycolytic flux, as evidenced by reduced lactate production, and strongly inhibited carbonic anhydrase (CA) esterase activity. Molecular docking analyses provided structural insights, demonstrating credible binding of Albendazole to β-tubulin and Etoricoxib to Carbonic Anhydrase IX (CA-IX), thereby supporting a dual-targeting strategy aimed at disrupting the "Growth Hub" and "Power Hub" of cancer cells.

Our findings highlight the strong synergy between Albendazole and Etoricoxib, as evidenced by decreased IC_{50} values from high levels in monotherapy to significantly lower concentrations when combined. The combination shows time-dependent potency, with CI values indicating 'Very Strong Synergism' (CI < 0.1), and high DRI values suggest effective dose reduction, which could reduce toxicity. Additionally, the combination shows notable selectivity, with the SI increasing over time, whereas 5-FU shows a decreasing SI. Morphological assessments confirmed that apoptosis occurs specifically in cancer cells, sparing normal fibroblasts, emphasizing the potential to exploit cancer-specific metabolic vulnerabilities for therapeutic advantage.

The cytotoxic mechanisms of albendazole and etoricoxib, along with their potential synergy in cancer treatment, can be thoroughly understood by reviewing existing research on their individual anticancer actions. Historically, albendazole's anticancer potential has been attributed to its well-known microtubule-disrupting activity. As a benzimidazole compound, it binds to β-tubulin, prevents polymerization, and causes mitotic arrest and apoptosis [17, 18]. However, emerging research indicates that albendazole's influence may extend beyond its effects on cytoskeletal dynamics. Specifically, it has been demonstrated to induce mitochondrial dysfunction, leading to increased intracellular reactive oxygen species (ROS) and disruption of cellular energy metabolism [25, 48, 49]. This statement supports the hypothesis that microtubules function beyond structural support, playing a crucial role in intracellular trafficking. These processes include the transport of glucose transporters and the assembly of glycolytic enzymes into metabolons to enhance metabolic efficiency [25, 26]. Therefore, the mechanism of Albendazole can be interpreted as a dual-targeted approach that affects both the "Growth Hub" (cell division) and the "Power Hub" (energy production) by disrupting their respective functions.

Etoricoxib, a selective inhibitor of cyclooxygenase-2 (COX-2), has been shown to possess off-target antineoplastic properties that are independent of its primary anti-inflammatory effects. COX-2 overexpression is a common feature of various malignancies, and its inhibition can suppress tumor proliferation and angiogenesis. Nevertheless, its role within the proposed mechanism is complex and multifaceted. Recent research indicates an interaction between inflammatory signaling pathways and tumor metabolic processes. Notably, some COX-2 inhibitors have been reported to modulate cellular pH homeostasis [22, 24]. A vital aspect of tumor biology is regulated by enzymes such as Carbonic Anhydrase IX (CA-IX). [39, 40]. CA-IX is a hypoxia-inducible enzyme that catalyzes the hydration of CO_2, facilitating acid extrusion to maintain a conducive intracellular pH while acidifying the extracellular matrix to promote invasion and metastasis [47].

Furthermore, by building on previously proposed mechanisms, our metabolic assays providea critical exploration of the mixture's anticancer activity and the synergistic anticancer pattern among its ingredients, showing that the drug combination synergistically inhibits lactate production, implying a catastrophic disruption of glycolytic flux. Although Albendazole alone demonstrated a significant anti-glycolytic effect, its efficacy was substantially enhanced when combined with Etoricoxib. This suggests that Albendazole's disruption of microtubule-based transport impairs the cell's capacity to effectively mobilize glycolytic machinery, thereby increasing the cell's sensitivity to Etoricoxib's metabolic inhibition.

Targeting lactate production is a promising therapeutic approach that disrupts the fundamental metabolic vulnerability characteristic of cancer cells. Many malignancies exhibit the Warburg effect, relying

heavily on increased glycolytic flux and lactate production for energy and biosynthesis even under normal oxygen levels [50]. Therapeutic inhibition of lactate production, exemplified by targeting lactate dehydrogenase A (LDHA) or the monocarboxylate transporter 4 (MCT4), directly disrupts this metabolic reprogramming [51]. The result is a profound bioenergetic and biosynthetic crisis that impairs ATP production and the synthesis of macromolecules essential for rapid cellular proliferation [52]. Furthermore, the accumulation of glycolytic intermediates may induce toxic metabolic stress. Additionally, disrupting the lactate-rich tumor microenvironment can impair immune evasion and metastatic potential, thereby promoting selective apoptosis of cancer cells [53].

Furthermore, our metabolic assays demonstrated significant suppression of carbonic anhydrase esterase activity, primarily induced by Etoricoxib, with an enhanced effect observed when combined. This suggests a considerable impairment of the cancer cell's primary pH-regulation mechanism. Inhibition of carbonic anhydrase (CA), especially the tumor-associated CA-IX isoform, is a promising therapeutic approach to disrupt a vital survival pathway in cancer cells. CA-IX plays a critical role in maintaining pH homeostasis by catalyzing the hydration of CO_2, thereby facilitating proton extrusion and acidifying the extracellular tumor microenvironment. This microenvironment promotes tumor invasion, metastasis, and chemotherapy resistance, underscoring the potential impact of targeting CA-IX in cancer treatment [22, 24]. Inhibition of this enzymatic activity, thereby impairing pH regulation, results in intracellular acidification [47]. This metabolic stress, in conjunction with additional insults such as glycolytic inhibition, has the potential to induce a lethal bioenergetic crisis. This mechanism selectively targets cancer cells that depend heavily on carbonic anhydrase IX (CA-IX) for survival in hypoxic, acidic microenvironments [53-56].

This dual mechanism—entailing the concurrent inhibition of glycolytic energy production and disruption of pH homeostasis—ultimately results in an insurmountable bioenergetic crisis, herein designated "energetic strangulation."

The molecular docking results offer a solid structural explanation for our metabolic assay findings. Notably, the binding of albendazole to the human wild-type β-tubulin subunit, indicated by a favorable docking score and specific interactions with residues such as ASN A:206 and TYR A:224, supports its well-known microtubule-disrupting activity. Additionally, the docking of etoricoxib within the active site of carbonic anhydrase IX (CA-IX), involving multiple hydrogen bonds with key residues including ARG A:196 and ASN A:198, suggests a new direct mechanism. This indicates that etoricoxib may act as a CA-IX inhibitor, directly blocking the tumor's ability to control metabolic acidosis driven by increased glycolytic activity. The inhibition of CA-IX by Etoricoxib represents a noteworthy secondary mechanism. While primarily recognized for its COX-2 inhibitory activity, the molecular docking and enzymatic studies presented here indicate a direct off-target interaction with CA-IX. This finding extends the known pharmacological profile of Etoricoxib, as direct CA-IX inhibition is not frequently reported. Such a discovery positions Etoricoxib as a multi-target agent in this therapeutic context, capable of modulating both inflammatory pathways and pH regulation, thereby disrupting cancer cell energetics. Although the binding affinity of Etoricoxib for CA-IX was marginally lower than that of the reference inhibitor SLC-0111, its biological efficacy was enhanced when combined with Albendazole, suggesting the potential for synthetic lethality in this combinatorial approach.

Despite promising findings, this study has notable limitations. Although the pharmacokinetics and safety profiles of both albendazole and etoricoxib are well documented, concerns remain about *in vitro* conditions. These conditions cannot fully replicate the complexities of the tumor microenvironment, pharmacokinetics, or immune interactions inherent in *in vivo* systems. Therefore, further validation using animal models is necessary.

CONCLUSION

This study tackles the significant issues of chemoresistance and limited selectivity in traditional cervical cancer treatments by exploring a new drug repurposing method. The combination of Albendazole and Etoricoxib exhibited strong synergistic cytotoxic effects against HeLa cervical cancer cells, substantially exceeding those of the standard chemotherapy drug 5-fluorouracil (5-FU).

This synergism was achieved through a mechanistically coherent, dual-target strategy: Albendazole weakened the structural integrity by targeting β -tubulin and reducing glycolytic activity, while Etoricoxib inhibited Carbonic Anhydrase and disrupted cellular pH regulation. Importantly, this

combination caused a selective "energetic deprivation' in cancer cells, leading to metabolic collapse and apoptosis, while sparing non-malignant fibroblasts.

Another support for this finding comes from in silico molecular docking results, which showed that albendazole and etoricoxib can target each β-tubulin subunit and the enzyme Carbonic Anhydrase IX, with docking scores of -6.7 and -7.1 kcal/mol, respectively. These findings indicate a promising therapeutic approach with a mechanistic rationale and the potential to overcome current treatment limitations, thereby justifying further preclinical investigation of this repurposed drug combination.

To translate these promising *in vitro* findings into clinical application, immediate subsequent steps are necessary. Validation across a diverse panel of cervical cancer cell lines, including those resistant to chemotherapy, would establish broader efficacy. Following this, *in vivo* studies utilizing cervical cancer xenograft models are crucial to assess the pharmacokinetics, tolerability, and antitumor activity of the combination within a complex tumor microenvironment, thereby directly supporting progression toward preclinical development.

AUTHOR CONTRIBUTIONS

Conceptualization: Aiad Gaber Arean, Sura Findakly. Azal hamoody jumaa

Methodology: Azal hamoody jumaa .Aiad Gaber Arean, Sura Findakly, Henan Dh. Skheel Aljebori.

Software: Aiad Gaber Arean.Azal hamoody jumaa

Validation: Saba Jesem Alheshemi, Sura Findakly. Azal hamoody jumaa

Formal Analysis: Azal hamoody jumaa .Aiad Gaber Arean, Henan Dh. Skheel Aljebori.

Investigation: Saba Jesem Alheshemi, Sura Findakly. Azal hamoody jumaa

Resources: Sura Findakly.

Data Curation: Saba Jesem Alheshemi.Azal hamoody jumaa

Writing – Original Draft: Saba Jesem Alheshemi. Azal hamoody jumaa

Writing – Review & Editing: Sura Findakly, Aiad Gaber Arean.

Visualization: Aiad Gaber Arean.Azal hamoody jumaa

Supervision: Sura Findakly, Aiad Gaber Arean.

Project Administration: Sura Findakly.

ACKNOWLEDGEMENTS

The research team sincerely extends its heartfelt gratitude to the researchers and instructional staff at ICMGR/Al-Mustansiriyah University and the Iraqi National Cancer Research Centre/University of Baghdad for their invaluable support throughout this study. We are also very thankful to the dedicated quality control team at Samarra Pharmaceutical Factory for providing the essential drugs used in our research.

FINANCIAL SUPPORT AND SPONSORSHIP

Self-funded

CONFLICTS OF INTEREST

The authors formally declare that there are no conflicts of interest to disclose.

ABBREVIATIONS

5-FU = 5-Fluorouracil

MTT = 3-(4,5-Dimethylthiazol-2-yl)-2,5-diphenyltetrazolium bromide

CI = Combination Index

DRI = Dose Reduction Index

CA = Carbonic Anhydrase

CA-IX = Carbonic Anhydrase IX

COX-2 = Cyclooxygenase-2

MEM = Minimum Essential Medium

FBS = Fetal Bovine Serum

HFF = Human Foreskin Fibroblasts

DMSO = Dimethyl Sulfoxide

SD = Standard Deviation

ANOVA = Analysis of Variance

LSD = Least Significant Difference

4-NPA = 4-Nitrophenyl Acetate

PBS = Phosphate-Buffered Saline

BCA = Bicinchoninic Acid

PDB = Protein Data Bank

SI = Selective Index

ROS = Reactive Oxygen Species

LDHA = Lactate Dehydrogenase A

MCT4 = Monocarboxylate Transporter 4

ATP = Adenosine Triphosphate

HIF-1α = Hypoxia-Inducible Factor 1-alpha

GLUT4 = Glucose Transporter Type 4

SPSS = Statistical Package for the Social Sciences

IC_{50} = Half Maximal Inhibitory Concentration

REFERENCES

[1] Sung H, Ferlay J, Siegel RL, Laversanne M, Soerjomataram I, Jemal A, *et al*. Global cancer statistics 2020: GLOBOCAN estimates of incidence and mortality worldwide for 36 cancers in 185 countries. CA: A Cancer Journal for Clinicians 2021; 71(3): 209-49. https://doi.org/10.3322/caac.21660

[2] Singh D, Vignat J, Lorenzoni V, Eslahi M, Ginsburg O, Lauby-Secretan B, *et al*. Global estimates of incidence and mortality of cervical cancer in 2020: a baseline analysis of the WHO Global Cervical Cancer Elimination Initiative. The Lancet Global Health 2023; 11(2): e197-e206. https://doi.org/10.1016/S2214-109X(22)00501-0

[3] Abdulla KN, Aljebori S, Dh H, Mohson KI, Sabah Rasoul N, Mahdi MA. Risk factors for cervical cancer in Iraqi women. Libri Oncologici: Croatian Journal of Oncology 2023; 51(2-3): 59-64. https://doi.org/10.20471/LO.2023.51.02-03.09

[4] Shahzad A, ur Rehman A, Naz T, Rasool MF, Saeed A, Rasheed S, *et al*. Addition of Bevacizumab to Chemotherapy and Its Impact on Clinical Efficacy in Cervical Cancer: A Systematic Review and Meta-Analysis. Pharmacy 2024; 12(6): 180. https://doi.org/10.3390/pharmacy12060180

[5] Abdulla KN, Khashman BM, Alheshimi SJ. The Immunohistochemical Evaluation of BRCA2 Expression with HPV Infection in a Group of Iraqi Women with Cervical Carcinoma. Indian Journal of Public Health Research & Development 2019; 10(9). https://doi.org/10.5958/0976-5506.2019.02590.7

[6] Pangarkar K. Development of cisplatin as an anti-cancer drug 2025.

[7] Masuda T, Tsuruda Y, Matsumoto Y, Uchida H, Nakayama KI, Mimori K. Drug repositioning in cancer: The current situation in Japan. Cancer Science 2020; 111(4): 1039-46. https://doi.org/10.1111/cas.14318

[8] Wieder R, Adam N. Drug repositioning for cancer in the era of AI, big omics, and real-world data. Critical Reviews in Oncology/Hematology 2022; 175: 103730. https://doi.org/10.1016/j.critrevonc.2022.103730

[9] Yousif BJ, Abd Alwahab DH, Mohammed HA, Yasin YS, Jumaa AH. Antiproliferative Potential of Linagliptin-Rivaroxaban Mixture in Cervical Cancer: Mechanistic Insights into Targeting Mutant MAPK, RAS kinase Signal Protein. Asian Pacific Journal of Cancer Prevention 2025; 26(8): 3053-64. https://doi.org/10.31557/APJCP.2025.26.8.3053

[10] Salih SR, Abdulla KN, K Awn A, Yasin YS, Jumaa AH. Impact of Esomeprazole, Ciprofloxacin and Their Combination on Cervical Cancer Cell Line Proliferation: A Focus on Heat Shock Protein 70 Modulation. Asian Pacific Journal of Cancer Prevention 2025; 26(7): 2455-66. https://doi.org/10.31557/APJCP.2025.26.7.2455

[11] Al-Mahdwi TT, Said AM, Hade IM, Yasin YS, Jumaa AH. Synergistic Cytotoxic Impact of Linagliptin-Ciprofloxacin Combination on Cervical Cancer Cell Line: Insights into Targeting Heat Shock Protein 60. Asian Pacific Journal of Cancer Prevention: APJCP 2025; 26(6): 2117. https://doi.org/10.31557/APJCP.2025.26.6.2117

[12] Abdulla KN, Khudhur RK, Said AM, Jumaa AH, Yasin YS. Laetrile and Methotrexate: A Dual-Drug Approach to Inhibiting Cervical Cancer Cell Proliferation. Journal of Cancer Research Updates 2025; 14: 52-62. https://doi.org/10.30683/1929-2279.2025.14.06

[13] Ahmed A, Nihad A, Sabreen G, Yasin YS, Azal J. Synergistic Antiproliferative Effect of Linagliptin-Metformin Combination on the Growth of Hela Cancer Cell Line. Journal of Cancer Research Updates 2025; 14: 12-23. https://doi.org/10.30683/1929-2279.2025.14.02

[14] Jumaa AH, Hade IM, Abdulla KN, Yasin YS. Ciprofloxacin and Metformin as Dual Therapeutic Agents: Synergistic Impact on Cervical Cancer Cell line Proliferation: Insight into Cytoplasmic SRC Tyrosine Kinase Targeting. Asian Pacific Journal of Cancer Biology 2025; 10(3): 699-712. https://doi.org/10.31557/apjcb.2025.10.3.699-712

[15] Khudhur RK, Yahiya YI, Majeed AH, Yasin YS, Jumaa AH. Scrutiny of the Co-Cytotoxic Impact of Metformin-Omeprazole on the Cervical Cancer Cell Line and Their Aptitude to Target Heat Shock 60. Asian Pacific Journal of Cancer Prevention: APJCP 2025; 26(4): 1353. https://doi.org/10.31557/APJCP.2025.26.4.1353

[16] Hashim WS, Yasin YS, Jumaa AH, Al-Zuhairi MI, Abdulkareem AH. Physiological Scrutiny to Appraise a Flavonol Versus Statins. Biomedical and Pharmacology Journal 2023; 16(1): 289-93. https://doi.org/10.13005/bpj/2610

[17] Chai J-Y, Jung B-K, Hong S-J. Albendazole and mebendazole as anti-parasitic and anti-cancer agents: an update. The Korean journal of parasitology 2021; 59(3): 189. https://doi.org/10.3347/kjp.2021.59.3.189

[18] Liu H, Sun H, Zhang B, Liu S, Deng S, Weng Z, *et al*. 18F-FDG PET imaging for monitoring the early anti-tumor effect of albendazole on triple-negative breast cancer. Breast Cancer 2020; 27(3): 372-80. https://doi.org/10.1007/s12282-019-01027-5

[19] Enkai S, Kouguchi H, Inaoka DK, Irie T, Yagi K, Kita K. *In vivo* efficacy of combination therapy with albendazole and atovaquone against primary hydatid cysts in mice. European Journal of Clinical Microbiology & Infectious Diseases 2021; 40(9): 1815-20. https://doi.org/10.1007/s10096-021-04230-5

[20] Kumbhar P, Kole K, Manjappa A, Jha NK, Disouza J, Patravale V. Drug Repurposing Opportunities in Cancer. Drug Repurposing for Emerging Infectious Diseases and Cancer: Springer; 2023; pp. 53-87. https://doi.org/10.1007/978-981-19-5399-6_5

[21] Md S, Alhakamy NA, Alharbi WS, Ahmad J, Shaik RA, Ibrahim IM, *et al*. Development and evaluation of repurposed etoricoxib loaded nanoemulsion for improving anticancer

activities against lung cancer cells. International Journal of Molecular Sciences 2021; 22(24): 13284. https://doi.org/10.3390/ijms222413284

[22] Almansour NM. Computational Discovery of Selective Carbonic Anhydrase IX (CA IX) Inhibitors via Pharmacophore Modeling and Molecular Simulations for Cancer Therapy. International Journal of Molecular Sciences 2025; 26(17): 8465. https://doi.org/10.3390/ijms26178465

[23] Yousif BJ, Alwahab A, Hassan D, Mohammed HA, Yasin YS, Jumaa AH. Antiproliferative Potential of Linagliptin-Rivaroxaban Mixture in Cervical Cancer: Mechanistic Insights into Targeting Mutant MAPK, RAS kinase Signal Protein. Asian Pacific Journal of Cancer Prevention 2025; 26(8): 3053-64. https://doi.org/10.31557/APJCP.2025.26.8.3053

[24] Daunys S, Petrikaitė V. The roles of carbonic anhydrases IX and XII in cancer cell adhesion, migration, invasion and metastasis. Biology of the Cell 2020; 112(12): 383-97. https://doi.org/10.1111/boc.201900099

[25] Liu Y-J, Chang Y-J, Kuo Y-T, Liang P-H. Targeting β -tubulin/CCT-β complex induces apoptosis and suppresses migration and invasion of highly metastatic lung adenocarcinoma. Carcinogenesis 2020; 41(5): 699-710. https://doi.org/10.1093/carcin/bgz137

[26] Lu W, Shen L, Zhao S. Integrated in silico-*in vitro* profiling of the systematic response of paclitaxel and its analogues to clinical tubulin variations in gynecologic cancers: Implications for the molecular mechanism of acquired tumor chemoresistance. Journal of the Chinese Chemical Society 2025; 72(1): 14-26. https://doi.org/10.1002/jccs.202400259

[27] Jarad A. Diabetic wound healing enhancement by tadalafil 2020.

[28] Saboowala HK. What HeLa Cells aka Immortal Cells Are and Why They Are Important. An Example of Racism in Medicine: Dr. Hakim Saboowala; 2022.

[29] Lyapun I, Andryukov B, Bynina M. HeLa cell culture: Immortal heritage of henrietta lacks. Molecular Genetics, Microbiology and Virology 2019; 34(4): 195-200. https://doi.org/10.3103/S0891416819040050

[30] Nadalutti CA, Wilson SH. Using human primary foreskin fibroblasts to study cellular damage and mitochondrial dysfunction. Current Protocols in Toxicology 2020; 86(1): e99. https://doi.org/10.1002/cptx.99

[31] Souren NY, Fusenig NE, Heck S, Dirks WG, Capes-Davis A, Bianchini F, *et al*. Cell line authentication: a necessity for reproducible biomedical research. The EMBO Journal 2022; 41(14): e111307. https://doi.org/10.15252/embj.2022111307

[32] Arunachalam K, Sreeja PS. MTT Assay Protocol. Advanced Cell and Molecular Techniques: Protocols for *In vitro* and *In vivo* Studies: Springer; 2025. p. 271-6. https://doi.org/10.1007/978-1-0716-4518-5_45

[33] Yasin Al-Samarray YS, Jumaa AH, Hashim WS, Khudhair yi. The cytotoxic effect of ethanolic extract of cnicus benedictus l. Flowers on the murine mammary adenocarcinoma cancer cell line amn-3. Biochemical & Cellular Archives 2020; 20.

[34] Le Berre M, Gerlach JQ, Dziembała I, Kilcoyne M. Calculating half maximal inhibitory concentration (IC 50) values from glycomics microarray data using graphpad prism. Glycan Microarrays: Methods and Protocols 2022: 89-111. https://doi.org/10.1007/978-1-0716-2148-6_6

[35] He Y, Zhu Q, Chen M, Huang Q, Wang W, Li Q, *et al*. The changing 50% inhibitory concentration (IC50) of cisplatin: a pilot study on the artifacts of the MTT assay and the precise measurement of density-dependent chemoresistance in ovarian cancer. Oncotarget 2016; 7(43): 70803. https://doi.org/10.18632/oncotarget.12223

[36] Bezerra JN, Gomez MCV, Rolón M, Coronel C, Almeida-Bezerra JW, Fidelis KR, *et al*. Chemical composition, Evaluation of Antiparasitary and Cytotoxic Activity of the essential oil of Psidium brownianum MART EX. DC. Biocatalysis and Agricultural Biotechnology 2022; 39: 102247. https://doi.org/10.1016/j.bcab.2021.102247

[37] Meyer CT, Wooten DJ, Lopez CF, Quaranta V. Charting the Fragmented Landscape of Drug Synergy. Trends Pharmacol Sci 2020; 41(4): 266-80. https://doi.org/10.1016/j.tips.2020.01.011

[38] Chou T-CJS. The combination index (CI< 1) as the definition of synergism and of synergy claims. Elsevier; 2018; pp. 49-50. https://doi.org/10.1016/j.synres.2018.04.001

[39] Wei S, Dai Z, Wu L, Xiang Z, Yang X, Jiang L, *et al*. Lactate-induced macrophage HMGB1 lactylation promotes neutrophil extracellular trap formation in sepsis-associated acute kidney injury. Cell Biology and Toxicology 2025; 41(1): 1-19. https://doi.org/10.1007/s10565-025-10026-6

[40] Rasheed S, ul Huda N, Fisher SZ, Falke S, Gul S, Ahmad MS, *et al*. Identification, crystallization, and first X-ray structure analyses of phenyl boronic acid-based inhibitors of human carbonic anhydrase-II. International Journal of Biological Macromolecules 2024; 267: 131268. https://doi.org/10.1016/j.ijbiomac.2024.131268

[41] Salentin S, Schreiber S, Haupt VJ, Adasme MF, Schroeder MJNar. PLIP: fully automated protein–ligand interaction Profiler 2015; 43(W1): W443-W7. https://doi.org/10.1093/nar/gkv315

[42] Chen G, Seukep AJ, Guo MJMd. Recent advances in molecular docking for the research and discovery of potential Marine Drugs 2020; 18(11): 545. https://doi.org/10.3390/md18110545

[43] Rahayu NI, Muktiarni M, Hidayat Y. An application of statistical testing: A guide to basic parametric statistics in educational research using SPSS. ASEAN Journal of Science and Engineering 2024; 4(3): 569-82. https://doi.org/10.17509/ajse.v4i3.76092

[44] Mahdi HM, Wadee SA. Interaction Effect of Methotrexate and Aspirin on MCF7 cell line Proliferation: *In vitro* Study. Journal of Advanced Veterinary Research 2023; 13(9): 1767-71.

[45] Guo L-Y, Xing X, Tong J-B, Li P, Ren L, An C-X. Qsar Aided Design of Potent Ret Inhibitors Using Molecular Docking, Molecular Dynamics Simulation and Binding Free Energy Calculation. Molecular Dynamics Simulation and Binding Free Energy Calculation 2024. https://doi.org/10.2139/ssrn.4886845

[46] Fang S, Bi S, Li Y, Tian S, Xu H, Wang S, *et al*. Design, synthesis and anti-tumor evaluation of plinabulin derivatives as potential agents targeting β -tubulin. Bioorganic & Medicinal Chemistry Letters 2023; 91: 129370. https://doi.org/10.1016/j.bmcl.2023.129370

[47] Supuran CT. Carbonic anhydrase inhibitors: an update on experimental agents for the treatment and imaging of hypoxic tumors. Expert Opinion on Investigational Drugs 2021; 30(12): 1197-208. https://doi.org/10.1080/13543784.2021.2014813

[48] Fatima I, Ahmad R, Barman S, Gowrikumar S, Pravoverov K, Primeaux M, *et al*. Albendazole inhibits colon cancer progression and therapy resistance by targeting ubiquitin ligase RNF20. British Journal of Cancer 2024; 130(6): 1046-58. https://doi.org/10.1038/s41416-023-02570-x

[49] Hashim WS, Jumaa AH, Alsaadi NT, Arean AG. Physiological Study Comprising the Sequelae of Magnetic Radiation on Human. Indian Journal of Forensic Medicine & Toxicology 2020; 14(2): 421-5.

[50] Hanahan D. Hallmarks of cancer: new dimensions. Cancer Discovery 2022; 12(1): 31-46. https://doi.org/10.1158/2159-8290.CD-21-1059

[51] Vaupel P, Schmidberger H, Mayer A. The Warburg effect: essential part of metabolic reprogramming and central contributor to cancer progression. International Journal of Radiation Biology 2019; 95(7): 912-9. https://doi.org/10.1080/09553002.2019.1589653

[52] Liberti MV, Locasale JW. The Warburg effect: how does it benefit cancer cells? Trends in Biochemical Sciences 2016; 41(3): 211-8. https://doi.org/10.1016/j.tibs.2015.12.001

[53] Barba I, Carrillo-Bosch L, Seoane J. Targeting the Warburg effect in cancer: where do we stand? International Journal of Molecular Sciences 2024; 25(6): 3142. https://doi.org/10.3390/ijms25063142

[54] Ibraheem MA, Elfakharany EM, Moussa S, Mohammed FA-r. An overview on Hyaluronidase enzyme types, mode of action, assay and therapeutic applications. Journal of Scientific Research in Science 2024; 41(2): 1-17. https://doi.org/10.21608/jsrs.2024.273369.1125

[55] Sakr DE, Abdelsattar M, Hathout TA, Hassanein SE, Abdelgawad ZA. Improvement of inulin production in Jerusalem artichoke (Helianthus tuberosus L.) through foliar application of certain sugars. Journal of Scientific Research in Science 2024; 41(2): 18-46. https://doi.org/10.21608/jsrs.2024.265530.1124

[56] Dawood YJ, Mahdi MA, Jumaa AH, Saad R, Khadim RM. Evaluation of LH, FSH, oestradiol, prolactin and tumour markers CEA and CA-125 in sera of Iraqi patients with endometrial cancer. Scripta Medica 2024; 55(4): 419-26. https://doi.org/10.5937/scriptamed55-49925

Received on 07-12-2025 Accepted on 06-01-2026 Published on 30-01-2026

https://doi.org/10.30683/1929-2279.2026.15.03